International Journal of Electrical and Computer Engineering (IJECE)
Vol. 9, No. 6, December 2019, pp. 4493~4506
ISSN: 2088-8708, DOI: 10.11591/ijece.v9i6.pp4493-4506

Variable structure control for an isolated boost converter used in fuel cell applications

S. Vijaya Madhavi, G. Tulasi Ram Das
Department of Electrical and Electronics Engineering, Jawaharlal Nehru Technological University, India

Article Info

Article history:

Received Oct 24, 2018
Revised Jun 24, 2019
Accepted Jul 4, 2019

Keywords:

Fuel cells
Isolated full bridge boost converter
Sliding mode control
Variable structure theory

ABSTRACT

In recent years fuel cells have become prominent as an alternative source of energy to meet the society's energy requirements. A control strategy derived from variable structure theory known as Sliding Mode Control (SMC) was proposed for an Isolated Boost topology which was mostly used in fuel cell systems. Converter operation and its detailed mathematical modelling are also presented. Then the converter with the control strategy suggested is simulated in MATLAB/SIMULINK and compared with other controllers. The results show that transient response of the converter is very fast and steady state error is reduced throughout the load change period with proposed control topology.

Corresponding Author:

S. Vijaya Madhavi,
Departement of Electrical and Electronics Engineering,
Jawaharlal Nehru Technological University,
Hyderabad, Telangana, India.
Email: vijaya.madhavi83@gmail.com

1. INTRODUCTION

As fossil fuel reserves are exhausting, environment is polluted due to gas emissions and as energy demands are increasing an emergency situation arises to search for an alternative source of energy. As a result various renewable energy sources have been explored and Fuel cells arise as the most efficient alternative energy sources because of its advantages like refuel ability, producing very low emissions, portable in size, little maintenance etc. In spite of these benefits the price of fuel cell is its main constraint [1, 2]. Fuel cell is an electro chemical device which gives electricity by combining hydrogen and oxygen without any combustion producing water and heat. The output voltage of these fuel cells largely varies under variable load conditions and is also very low in magnitude. This low voltage must be raised to peak of the utility to interconnect fuel cells to grid. Therefore DC-DC converters which boost the voltage to the required level are necessary to connect fuel cells to utility loads.

Many models of DC-DC converters are mentioned in the previous survey papers which are acceptable for fuel cell applications. From the suggested topologies in the literature [3-5] Isolated Full Bridge topology was most efficient and acceptable for use in fuel cells. The main advantages of isolated full bridge topology are possibility of applying soft switching techniques, reasonable device voltage ratings, less transistor voltage and current stress, possibility of connecting devices in parallel to achieve desired power levels and high efficiency and galvanic isolation.

Under varying load and varying input voltage conditions DC-DC converters should provide regulated DC output voltage. Changes in time, temperature, pressure etc changes the values of the converter components. Applying of negative feedback in the form of a closed loop, regulation of DC voltage can be achieved. So the next task in designing a power conditioning system is developing a best controller meeting the requirements suitable for fuel cell applications.

Basically there are two types of controllers, Voltage control and current control. Vast majority of DC-DC converters are implemented using current mode controllers because of its advantages [6-9]. The basic performance of current control is as indicated in Figure 1.

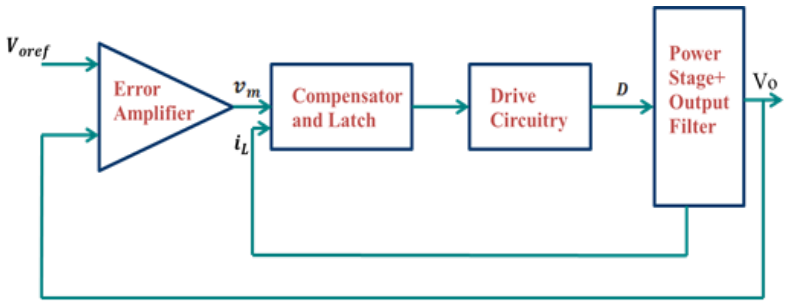

Figure 1. Implementation of current mode control

Here the output stage is fed by the inductor current i_L and the error voltage output from the error amplifier (known as control voltage) v_m controls it. This has an extreme effect on a dynamic behaviour of the negative feedback control loop. Using this approach many techniques are implemented like linear peak current control (LPCM), non-linear carrier control (NLC), predictive switching modulator (PSM) control etc. In the linear peak current control (LPCM) [10] peak switching current has to be sensed and therefore the sensing devices needed are more. In non-linear carrier current control (NLC) [11, 12] three reset integrators are needed to generate the carrier waveform. The NLC controlled converter results in distorted input current waveform in discontinuous conduction mode of operation.

To overcome the problems in LPCM and NLC controllers another control known as Predictive switching modulator control (PSM) [13-15] is proposed where only two reset integrators are used when compared to NLC. Also PSM [16, 17] control extends the range of continuous conduction mode as prediction of off state ripple current is possible which is added to on state actual current at the end of switching period. The transient reponse is also very slow with these controllers [18].

But the above methods of control require small signal representation of the system for an appropriate control to be developed and also the linear time invariant nature produces unpredicted action in the converter when running out of the normal operating point as small signal parameters strongly depend on it. Therefore to improve the transient reponse by considering the stability of the system in any case and its static and dynamic performances a control method should be developed. The control should also ensure not to accept disturbances in input voltage and effects of load variations. Generally the non-linear types of controllers are mostly used now days as they can meet the requirements of the control considering the uncertainties and non-linear state of the converter. This concept is obtained from the non-minimum phase character and variability in the structure of converters with unforeseeable non-linear change in the loads. As a result a robust control method was proposed based on variable structure theory taking into account the non-linear nature of the converters.

The introduction of variable structure system control popularly known as Sliding Mode control and its development was started in the early of 1950's in Soviet Union by Emelyanov and many co-researchers like Utkins and Itkis [19]. This method of control has many advantages as: excellent stability and Robustness for large input and output variations when compared to any other hysteresis control; as all the control loops are simultaneous, dynamic response of the system is very fast; execution of this control is very easy and not complicated; if N is the system state and N-1 is the state of system's response, then actually sliding mode have just N-1 independent state variables where N^{th} variable is restricted by sliding surface. The proposed control was applied to IFBC and simulated in MATLAB/SIMULINK. The obtained results were compared with LPCM, NLC and PSM controllers in terms of transient response parameters.

2. ISOLATED FULL BRIDGE BOOST CONVERTER TOPOLOGY (IFBC)

2.1. Basic converter operation

In this section complete working of the converter is presented. The converter circuit is represented by Figure 2 and its performance according to modes of operation is described by Figure 3.

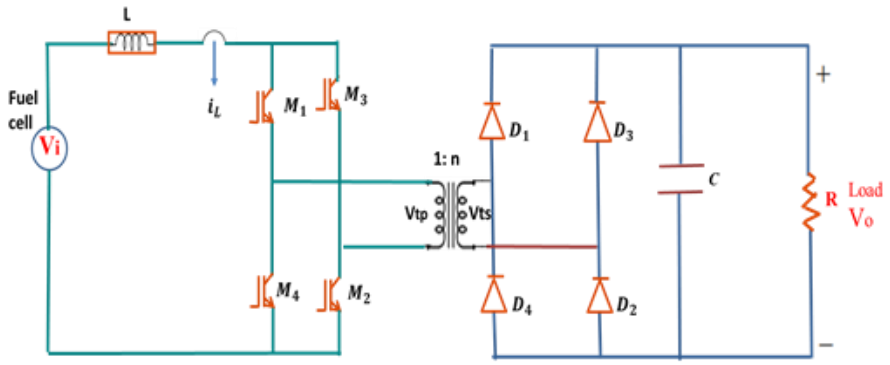

Figure 2. Isolated full bridge boost converter

Switches M1-M4 are run in pairs (i) M1-M2 and (ii) M3-M4 respectively. Switching pulses are 180 degrees phase shifted. Switch MOSFET duty cycle is chosen between 0.5 and 1 to ensure overlapping of switches [20].

- Mode1: During this period energy starts to distribute. Switches M1-M4 are in conduction. Input inductor L is charged by input power and transformer secondary voltage is zero. Secondary diodes are all in off state.
- Mode2: In this interval M1-M2 are in conduction and M3-M4 are in off state. Input power is allowed through M1-M2 and stored inductor energy is transferred to secondary side of transformer. Load power is achieved by conduction of diodes D1-D2.
- Mode3: This mode is same as mode1. All switches are in conduction and source inductor current rises gradually.
- Mode4: Reverse cycle period starts here. Switches M3-M4 are in conduction and M1-M2 are in off state. Discharging of source inductor energy and primary current transfer takes place through M3-M4 and transformer T1. Secondary current flow is achieved by conduction of diodes D3 and D4.

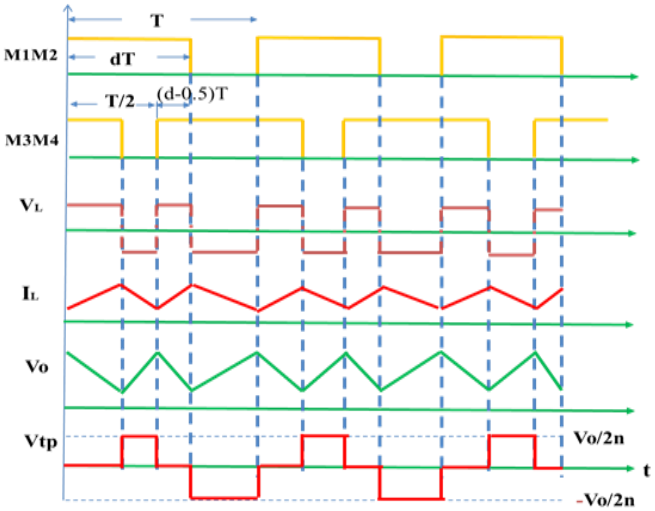

Figure 3. Basic operating waveforms of IFBC

3. SLIDING MODE CONTROL THEORY

This control is developed by utilizing concept of variable structure systems [21]. In these type of systems using a preset principle of control, system's actual composition is modified deliberately. The moments of modifying the structure can be resolved using current state of the system. This makes the Switching mode power supplies to fall into a specific category of VSS as its structure is modified regularly controlling operation of switches and diodes. In this process the structure of control system changes which indicates Variable structure control (VSC).

As VSC is a high speed switching feedback control it results in a Sliding mode. Based on a principle each feedback path gains shift between two values depending on the state value at each instant. The basis of the principle used which is also called as switching control law is to bring the non-linear system's trajectory on the surface in successive times. This surface is known as Switching Surface. The feedback path has a gain value if the plant's trajectory state is "above" this surface and it has a unique gain value when trajectory falls "below" the surface. Actual switching regulations are described by the surface. Perfectly speaking, control retains the trajectory state of the plant on the surface in successive times once obstructed. The plant dynamics confined to the surface indicate the performance of the system under control. The configuration of VSC can be split into two modules.

- In the first part a switching surface is chosen which makes the trajectory state of the plant confine to the surface and has required dynamics.
- In the second part a switching control law is modelled which moves the plant's state to switching surface and restricts to the surface on obstruction.

To specify the second part design, a lyapunov approach is used. In this approach a generalised lyapunov function which defines the trajectory state movement towards the surface is formed in terms of surface. The "gains" of each switched control structure is chosen such that the derivative of the lyapunov function is negative definite ensuring the movement of the trajectory state to the surface. This control is also known as Sliding Mode control highlighting the part of sliding mode. The variable structure control system may be formulated without a sliding mode, but such a system does not have related advantages.

3.1. Modelling of sliding mode system

Now consider a group of systems comprising state model with non-linear state vector x_s(t) and linear control vector u_c(t) in the form as [22]

$$\dot{x_s}(t) = \Phi(x_s, t, u_c) = \phi(x_s, t) + B(x_s, t)u_c(x_s,t) \quad (1)$$

Where t ϵ R^m and $B(x_s, t)$ ϵ R^{nXm} and furthermore every entry in $\phi(x_s, t)$ and $B(x_s, t)$ is supposed to be continuous with a bounded continuous derivative with respect to x_s.

A switching surface is chosen in the first module which makes trajectory state of plant confine to the surface and has required dynamics. Therefore by following the sliding mode control theory [14], the state variables of all areas are sensed and by using appropriate gains the states are multiplied and added together for the construction of sliding function ψ (x_s, t). The hysteresis block sustains this function to zero thereby the sliding surface can be outlined as

$$\psi(x_s, t) = \sum_1^N K_i x_{s_i} = 0 \quad (2)$$

Where N is the order of the system (i.e. count of state variables)

Considering second order system

$$\psi = x_{s_1} + \tau x_{s_2} \quad (3)$$

This is a linear combination of two state variables. The relation ψ = 0 indicates a line in phase plane which passes from origin (final equilibrium point of the system) and is called as sliding line.

Let us now specify the following control strategy

$$\text{If } \begin{matrix} \psi > +\epsilon \Rightarrow u_c = 0 \\ \psi > -\epsilon \Rightarrow u_c = 1 \end{matrix} \quad (4)$$

Where ϵ represents an appropriate hysteresis band. Likewise the phase plane is split to two regions partitioned with sliding line and individual region is related to one of the two sub topologies represented by switch position u_c.

- Position of the system continues to follow the phase trajectory as long as $u_c = 0$ when the system positions crosses the line $\psi = -\epsilon$ i.e. $u_c = 1$ based on equation.
- The system position continues to follow the phase trajectory as long as $u_c = 1$ when the system positions crosses the line $\psi = +\epsilon$ i.e. $u_c = 0$ based on equation

Looking at phase trajectories in closeness to sliding line, they are directed towards line only. Continuous commutations around the sliding line leads to motion which makes the system position drive to final equilibrium point. Based on the theory of a satisfactory small value of ϵ, two important resolutions are derived from the example.

- The system's progress is independent of its parameters when it is in sliding mode and depends only on chosen sliding line. Example in Figure 4 is system with first order dynamics and time constant equal to τ.
- Suppose order of the original system is N then system control dynamics in sliding mode possess order N-1 as the state variables are restricted by $\psi = 0$

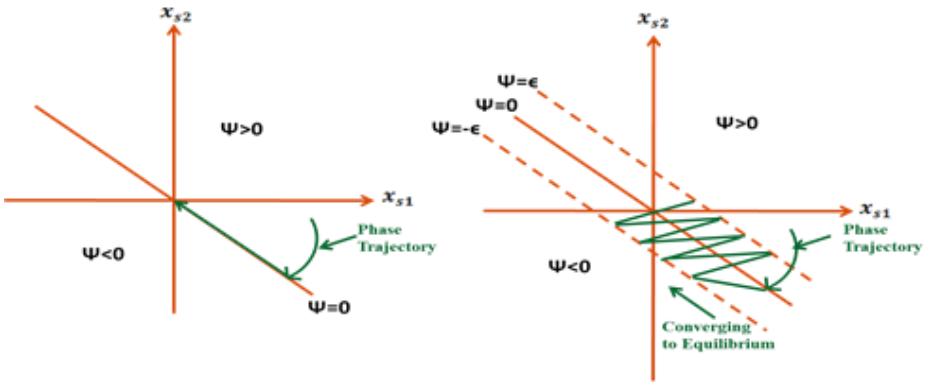

Figure 4. Sliding surface

Here using the amplitude of the hysteresis band ϵ switching frequency is derived. The abilities of the control technique are now visible for application in switched mode power supplies. Utilizing the inherent non-linear nature of these converters unlike to substructures constituting the system and its reduction dynamic performances are produced.

3.2. Modelling of switching surface

To model sliding mode control for the simple second order systems reviewed in previous section, choice of parameter τ is enough. Choice of this parameter should satisfy the following three constraints. Disregarding the starting point in phase plane system trajectories are needed to cross the sliding line which is known as *hitting condition.* The system trajectories which are near to the sliding line in both the regions are managed to run towards the line itself and is known as *existence condition.* The movement of system on sliding line (i.e. shifting towards equilibrium point) is regarded as *stability condition*.

3.3. Existence condition

In this condition the phase trajectories are needed to move towards sliding surface by little portion about the surface itself [23]. This is reached by interpreting a suitable Lyapunov function V (x_s, t, ψ). Generally it is appropriate to select a Lyapunov function of the form V $(x_s, t, \psi) = 0.5\psi^2(X)$. To deduce the required gains so that the system state drives to the surface $\psi(t) = 0$, one can select such that

$$\dot{V}(x_s, t, \psi) = 0.5\frac{d\psi^2}{dt} = \psi(X)\frac{d\psi(X)}{dt} = \psi.\dot{\psi} < 0 \quad (5)$$

So, when the distances to the surface and velocity of its change $\dot{\psi}$ are of opposite signs i.e. when $\lim_{x_{S\to+0}} \dot{\psi} > 0$ and $\lim_{x_{S\to+0}} \dot{\psi} < 0$ the sliding mode exists on a discontinuity surface.

3.4. Stability condition

Modelling of switching surface is estimated based on how the system understands its operation in sliding mode. The parameters of switching surface decide the system operation. If in any case attaining model of switching surface require logical reasoning describing the movement of state trajectory in sliding mode a method called Equivalent control is necessary for this description.

3.5. Equivalent control

This comprises an equivalent input and as the system stimulates, it provides system movement on sliding surface as long as the initial state is on. Let us assume that at time t_1 plant's state trajectory obstructs switching surface and a sliding mode exists. This indicates that, for all t $\geq t_1$, $\psi(x_s(t),t)=0$ and hence $\dot{\psi}(x_s(t),t)=0$. Utilizing chain rule [23], the equivalent control u_{ceq} for the system that can be interpreted as the input fulfils the condition

$$\dot{\psi}=\frac{\partial\psi}{\partial t}+\frac{\partial\psi}{\partial x_s}\dot{x_s}=\frac{\partial\psi}{\partial t}+\frac{\partial\psi}{\partial x_s}\varphi(x_s,t)+\frac{\partial\psi}{\partial x_s}B(x_s,t)u_{ceq}=0 \quad (6)$$

Supposing that the product matrix $\frac{\partial\psi}{\partial x_s}B(x_s,t)$ is non-singular for all t and x_s , one can calculate u_{ceq} as

$$u_{ceq}=-\left[\frac{\partial\psi}{\partial x_s}B(x_s,t)\right]^{-1}\left(\frac{\partial\psi}{\partial t}+\frac{\partial\psi}{\partial x_s}\varphi(x_s,t)\right) \quad (7)$$

Thus given $\psi(X_s(t_1))=0$ then for all t$\geq t_1$ the system dynamics on switching surface satisfies

$$\dot{x_s}(t)=\left[1-B(x_s,t)\left[\frac{\partial\psi}{\partial x_s}B(x_s,t)\right]^{-1}\frac{\partial\psi}{\partial x_s}\right]\varphi(x_s,t)-B(x_s,t)\left[\frac{\partial\psi}{\partial x_s}B(x_s,t)\right]^{-1}\frac{\partial\psi}{\partial t} \quad (8)$$

This shows dynamics of equivalent system on sliding surface. When some form of tracing or control is needed by the control system then the operating term is present. For example, when

$$\psi(x_s,t)=\sum_1^N K_i x_{si}+r(t)=0 \quad (9)$$

Where r(t) behaves as a "reference" signal.

3.6. Actual interpretation of equivalent control

A real control is that it always encompasses a slow component for which a high rate component is added. Therefore the control structure is decomposed as

$$u_c(x_s,t)=u_{ceq}(x_s,t)+u_{cN}(x_s,t) \quad (10)$$

In which u_{ceq} is valid only on sliding surface and u_{cN} satisfies actuality of sliding mode. Now u_{cN} is described as

$$u_{cN}(x_s,t)=sgn(\psi) \quad (11)$$

Where $sgn(\psi)=\frac{\psi}{|\psi|}$ (12)

The slow component indicates performance of the plant which is a dynamic device, but the plant's reaction to high rate component can be neglected. On the other side here there is need for interchange of actual control in the movement (12) with continuous function $u_{ceq}(x_s,t)$ that does not possess any high rate component. Thus the slow component of actual control which is the average control value is made equal therefore by using first order linear filter it can be estimated once the time constant is small in contrast with slow component, besides large enough so that high rate component can be filtered and can be roughly made equal with boundary layer width.

4. OUTPUT VOLTAGE REGULATION OF IFBC WITH SLIDING MODE CONTROL

By forcing the states to zero the regulation problem is resolved. In constructing the switching function, the nominal linear system representation is considered only when the matched uncertainty is present. Implementation IFBC with sliding mode control is depicted by Figure 5.

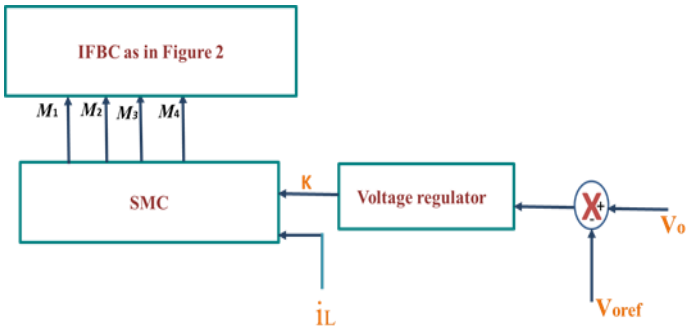

Figure 5. IFBC with sliding mode control

4.1. Modelling of the system

The closed loop dynamics of IFBC are represented by the following relations

$$\left.\begin{aligned} L\frac{di_L(t)}{dt} &= v_i(t) - \frac{1}{n}\big(1-u_c(t)\big)v_o(t) \\ C\frac{dv_o(t)}{dt} &= \frac{1}{n}\big(1-u_c(t)\big)i_L(t) - \frac{v_o(t)}{R} \end{aligned}\right\} \quad (13)$$

Where $u_c(t) = \begin{cases} 1, for\ 0 < t < dT \\ 0, for\ dT < t < T \end{cases}$

Here $u_c(t)$ is nothing but switch state or when average model is considered [24] it is the switch duty cycle and i_L, v_o are inductor current and output voltage of converter respectively. In sliding mode control $u_c(t)$ is described by the (4).

4.2. Average model of IFBC

As seen in section 2 operation of IFBC has two main intervals and their identical circuit diagrams are as shown in Figure 6.

- Interval 1: Here all the four switches M1-M4 conduct. The differential equations for this interval are written as

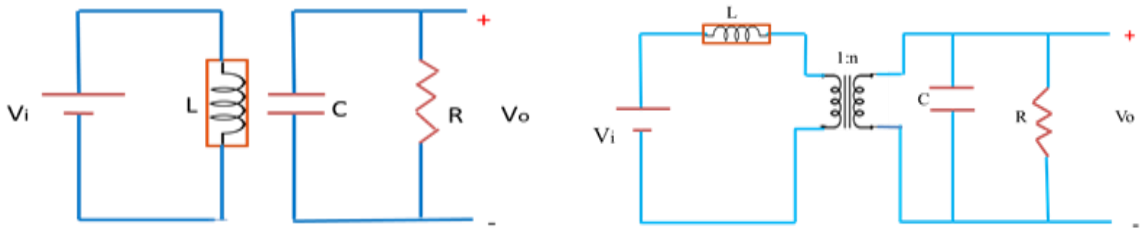

(a) (b)

Figure 6. Equivalent circuit with all switches and two diagonal switches conducting, (a) Interval 1, (b) Interval 2

$$v_i = L\frac{di_L}{dt} \xrightarrow{yields} \frac{di_L}{dt} = \frac{1}{L}v_i \quad (14)$$

$$\frac{v_o}{R} + C\frac{dv_o}{dt} = 0 \xrightarrow{yields} \frac{dv_o}{dt} = \frac{-1}{RC}v_o \quad (15)$$

$$\begin{bmatrix} \frac{di_L}{dt} \\ \frac{dv_o}{dt} \end{bmatrix} = \begin{bmatrix} 0 & 0 \\ 0 & \frac{-1}{RC} \end{bmatrix}\begin{bmatrix} i_L \\ v_o \end{bmatrix} + \begin{bmatrix} \frac{1}{L} \\ 0 \end{bmatrix} v_i \quad (16)$$

This interval continues for (d-0.5) T where T=1/f is the on period and d=t_{on}/T is the effectual duty ratio and n is the turns ratio of the isolated transformer.

- Interval 2: In this the switches M1 and M2 are on. The differential relations of state variables for this interval are written as follows

$$-v_i + L\frac{di_L}{dt} + \frac{v_o}{n} = 0 \xrightarrow{yields} \frac{di_L}{dt} = \frac{1}{L}v_i - \frac{1}{nL}v_o \tag{17}$$

$$\frac{i_L}{n} = \frac{v_o}{R} + C\frac{dv_o}{dt} \xrightarrow{yields} \frac{dv_o}{dt} = \frac{1}{nC}i_L - \frac{1}{RC}v_o \tag{18}$$

$$\begin{bmatrix} \frac{di_L}{dt} \\ \frac{dv_o}{dt} \end{bmatrix} = \begin{bmatrix} 0 & \frac{-1}{nL} \\ \frac{1}{nC} & \frac{-1}{RC} \end{bmatrix} \begin{bmatrix} i_L \\ v_o \end{bmatrix} + \begin{bmatrix} \frac{1}{L} \\ 0 \end{bmatrix} v_i \tag{19}$$

$$\text{Y= } v_o = Y_o = \begin{bmatrix} 0 & 1 \end{bmatrix} \begin{bmatrix} i_L \\ v_o \end{bmatrix} + [0]v_i \tag{20}$$

This interval continues for (1-d) T. The state equation for output in both the operations is same as (20). On averaging the state equations acquired during half of the switching cycle, a relation which has the features of both the modes is obtained

$$\text{A} = \begin{bmatrix} 0 & \frac{-2(1-d)}{nL} \\ \frac{2(1-d)}{nc} & \frac{-1}{RC} \end{bmatrix} B = \begin{bmatrix} \frac{1}{L} \\ 0 \end{bmatrix} \tag{21}$$

$$\dot{X} = \begin{bmatrix} 0 & \frac{-2(1-d)}{nL} \\ \frac{2(1-d)}{nc} & \frac{-1}{RC} \end{bmatrix} \begin{bmatrix} i_L \\ v_o \end{bmatrix} + \begin{bmatrix} \frac{1}{L} \\ 0 \end{bmatrix} v_i \tag{22}$$

$$Y_o = CX + DU = \begin{bmatrix} 0 & 1 \end{bmatrix} \begin{bmatrix} i_L \\ v_o \end{bmatrix} + [0]v_i \tag{23}$$

Here d is the controlling parameter of the system and is same as u_c

4.3. Control model

The main intention of IFBC control is regulation of output voltage v_o to a reference value v_{oref}. The modelling of sliding mode controller begins with selection of sliding surface. Only when the current increases constantly the direct surface inclines to zero. For solving two loop control problem, generally a cascade control structure is employed. Output voltage loop produces the reference current from the voltage error and inner current loop restricts inductor current through sliding mode.

Controlling of output voltage of the converter satisfies stability and presence of sliding mode. As sliding mode is extremely a non-linear method, it is very tough to obtain the gain of voltage loop. Moreover, as SMC can be implemented only to regulate current, voltage loop will quickly respond for any high frequency phenomena and uncertainties in reference current. Therefore to enhance controller capability, sliding surface based control mode that includes output voltage is suggested. For the IFBC converter the system cannot be represented in canonical form as the derivative of output voltage V_o becomes a discontinuous variable. Therefore as state variables the inductor current and output voltage errors are selected

$$\left.\begin{aligned} x_{s1} &= i_L - i_{Lref} \\ x_{s2} &= V_o - V_{oref} \end{aligned}\right\} \tag{24}$$

Here the inductor current reference i_{Lref} relies upon operating point (input voltage and output power) of the converter.

4.4. Existence condition

The relations of the IFBC converter system in terms of x_{s1} and x_{s2} are written as

$$\dot{x_s} = Ax_s + B\widehat{u_c} + D \tag{25}$$

Where $\dot{x_s} = [\dot{x_{s1}} \quad \dot{x_{s2}}]^T$

$$\text{A} = \begin{bmatrix} 0 & \frac{-2}{nL} \\ \frac{2}{nc} & \frac{-1}{RC} \end{bmatrix} B = \begin{bmatrix} \frac{2(x_{s2}+V_{oref})}{nL} \\ \frac{-2(x_{s1}+i_{Lref})}{nC} \end{bmatrix} D = \begin{bmatrix} \frac{V_i}{L} - \frac{2}{nL}V_{oref} \\ \frac{-V_{oref}}{RC} + \frac{2}{nC}i_{Lref} \end{bmatrix} and\ \widehat{u_c} = 1 - u_c\,.$$

Suppose for a short time let the signal i_{Lref} is available and constant. The phase trajectories of the system are as shown in Figure 7 and the sliding line equation is as

$$\psi(x_s) = x_{s1} + kx_{s2} = C^T x_s = 0 \tag{26}$$

On selecting the control law (4) it is simply observed that both the existence and reaching conditions are fulfilled (the past one at least in a small region surrounding the origin). The sliding mode existence region is specified by the following inequalities from (4)

$$\delta_1(x_s) = -\frac{k}{RC}x_{s2} + \frac{V_i}{nL} - V_{oref}\frac{k}{RC} > 0\ for\ \psi(x_s) < 0 \tag{27}$$

$$\delta_2(x_s) = -\left(\frac{k}{RC} + \frac{1}{nL}\right)x_{s2} + \frac{k}{nC}x_{s1} + \frac{V_i - V_{oref}}{nL} - \frac{k}{nC}\left(\frac{V_{oref}}{R} - i_{Lref}\right) < 0\ for\ \psi(x_s) > 0 \tag{28}$$

The relations $\delta_1(x_s) = 0$ and $\delta_2(x_s) = 0$ describe two lines in phase plane and are as shown in Figure 8.

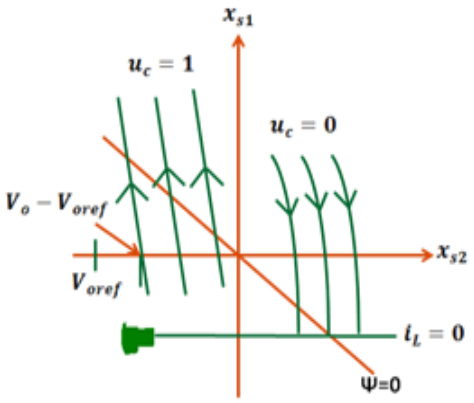

Figure 7. Phase trajectories and sliding line for IFBC

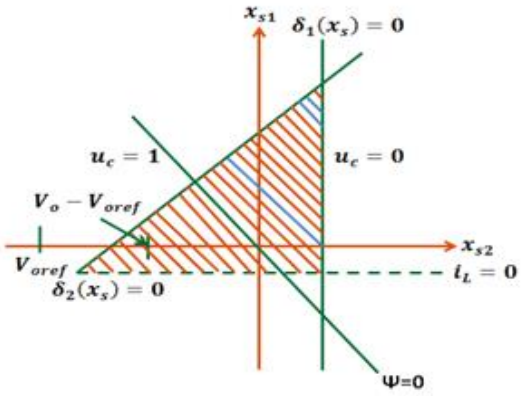

Figure 8. Existence regions in phase plane

One must make sure that both the intersections of the line $\delta_1(x_s) = 0$ with the x_{s2} axis and of $\delta_2(x_s) = 0$ with x_{s1} axis should be positive as can be seen to determine an existence region for sliding mode that involves origin (that shows the steady state point). This limitation from the above inequality determines the gain

$$k < \frac{RC}{nL}\frac{V_i}{V_{oref}} \tag{29}$$

To make sure the presence of sliding mode at least in a region about the steady state operating point, the coefficient of sliding surface is selected in such a way that it fulfils the (29). As the latter is based on the converter operating point (output power and input voltage), the presumption about availability of current reference signal i_{Lref} is not possible practically. Therefore to obtain this inductor current reference signal that controls the output voltage of converterV_o, generally a low-pass filter (or PI controller) is employed.

Obviously all the features of sliding control are considerably affected by this approach. At first owing to new state variable x_{s3}, the order of the system is increased by one. Therefore the whole system can be characterised by selecting the state variables as below

$$\left.\begin{matrix} x_{s1} = i_L \\ x_{s2} = V_o - V_{oref} \\ x_{s3} = \int x_{s2} dt \end{matrix}\right\} \tag{30}$$

$$\dot{x_s} = Ax_s + B\widehat{u_c} + D \tag{31}$$

Where $A = \begin{bmatrix} 0 & \frac{-2}{nL} & 0 \\ \frac{2}{nC} & -\frac{1}{RC} & 0 \\ 0 & 1 & 0 \end{bmatrix}$ $B = \begin{bmatrix} \frac{2V_o}{nL} \\ \frac{-2i_L}{nC} \\ 0 \end{bmatrix}$, $D = \begin{bmatrix} \frac{V_i}{L} - \frac{2}{nL}V_{oref} \\ \frac{-V_{oref}}{RC} + \frac{2}{nC}i_{Lref} \end{bmatrix}$

Now the sliding line turns into a sliding surface in phase space

$$\psi(x_s) = x_{s1} + kx_{s2} + \frac{1}{\tau}x_{s3} = C^T x_s = 0 \tag{32}$$

Here τ is time constant of low-pass filter and $C^T = \begin{bmatrix} 1 & k & \frac{1}{\tau} \end{bmatrix}$. Thus at steady state (32) the sliding surface produces zero output voltage error without considering operating point of converter [25].

4.5. Stability analysis

The system stability is possible only if the system dynamics in sliding rule provide path to the desired equilibrium point. It is suggested that only when the sliding regime is attained the dynamics of new state variables x_{s1}, x_{s2} and x_{s3} are obtained. For the system state to slide along the surface the equivalent average control should be implemented with the defined state space model (31), sliding surface (32) and $\dot{\psi}(x_s) = 0$ and is given by

$$u_{ceq} = 1 - \frac{\frac{V_i}{nL} + \frac{x_{s2}}{\tau} - \frac{k\left(x_{s2}+V_{oref}\right)}{RC}}{\frac{\left(x_{s2}+V_{oref}\right)}{nL} - \frac{kx_{s1}}{nC}} \tag{33}$$

So far as system stability is considered, applying positive values for coefficients of characteristic polynomial, we obtain

$$0 < k < k_{critc} = \frac{RC}{nL}\frac{V_i}{V_{oref}} \tag{34}$$

and

$$\tau > \frac{nL}{(1-D)^2 R} \frac{1}{1+\frac{2}{R(1-D)k}} \tag{35}$$

Thus the (34) and (35) represent the modelling relations for sliding mode control of IFBC converter that forces output voltage V_o to zero under steady state.

4.6. Switching frequency

Generally a practical system cannot be switched at infinite frequency, so a hysteresis band can be employed throughout the sliding line so that the switching frequency is settled at required value. Now by examining the Figure 9 the switching frequency can be evaluated

$$f_s = \frac{1}{\Delta t_1 + \Delta t_2} = \frac{1}{\alpha}\frac{f_N^- f_N^+}{f_N^+ - f_N^-} \tag{36}$$

$$f_N = C^T \dot{x_s} = \dot{\psi}(x_s) \tag{37}$$

Utilizing (6) and (10), (27) can be written as

$$f_s = \frac{c^T B}{\alpha} u_{ceq}(1 - u_{ceq}) \quad (38)$$

$$f_s = \frac{1}{\alpha n^2 CL} V_{oref} \left(1 - \frac{V_{oref}}{V_i}\right) \quad (39)$$

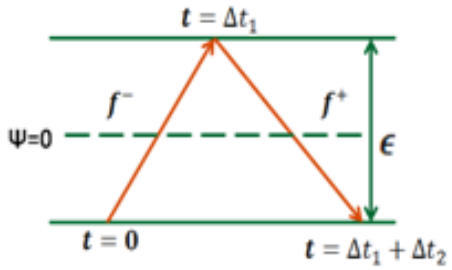

Figure 9. Details of system commutation with hysteresis

5. SIMULATION AND RESULTS

The Sliding mode control is modelled as stated in previous sections and is applied to IFBC converter. IFBC with SMC is simulated in MATLAB Simulink. The modeled sliding mode control block of IFBC and its sliding surface in MATLAB are as shown in Figure 10 and Figure 11 respectively. The converter specifications were given in Table 1. The output voltage of the converter is shown in Figure 12 with load change at 0.5sec and Figure 13 shows comparison of sliding mode control with PSM, NLC and LPCM controllers. Table 2 gives detailed performance analysis of IFBC with SMC, PSM, NLC and LPCM controllers.

Table 1. Design Specifications of IFBC

Specification	Value	Specification	Value
Output Power	1kw	Output Capacitor C	470µF
Input Fuel cell Voltage Vi	Fuel cell (6kw ,45V DC)	Load Resistor R	400ohms
Output Capacitor Voltage Vo	400V	Transformer voltage turns ratio	45:400
Input Inductor L	2.5mH	Switching frequency	10KHz

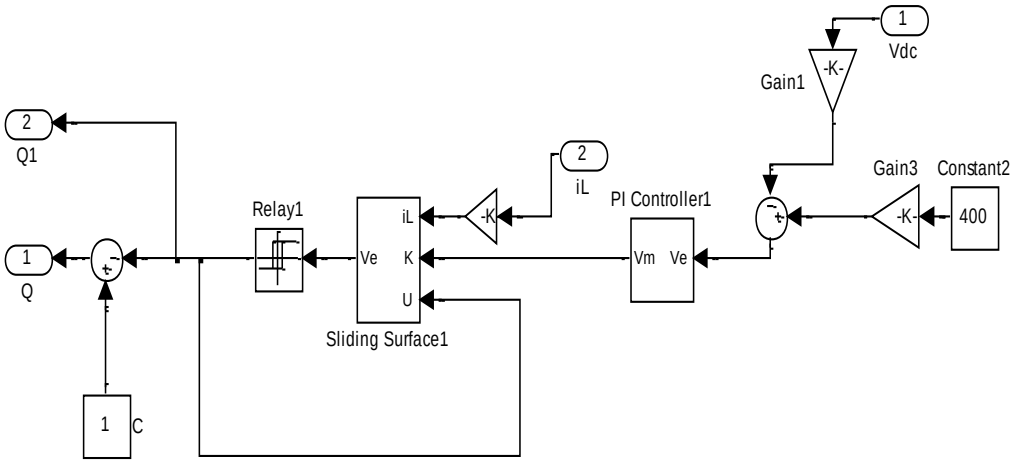

Figure 10. Simulink block of SMC

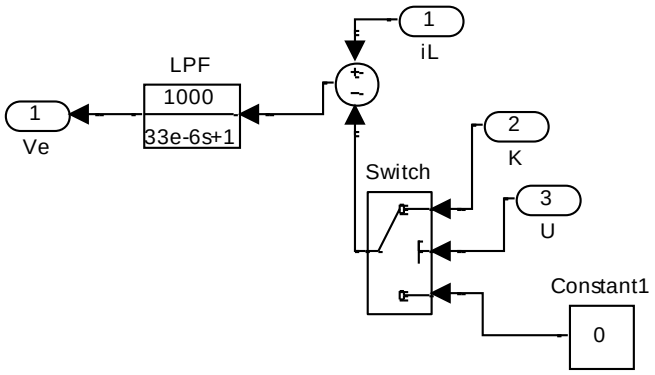

Figure 11. Simulink block of sliding surface

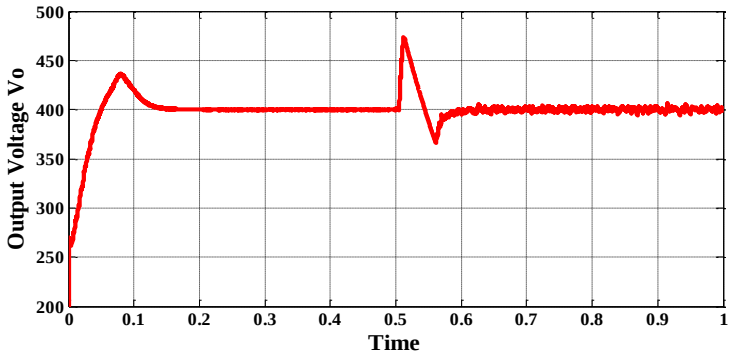

Figure 12. Output voltage of IFBC with SMC control for step change in load

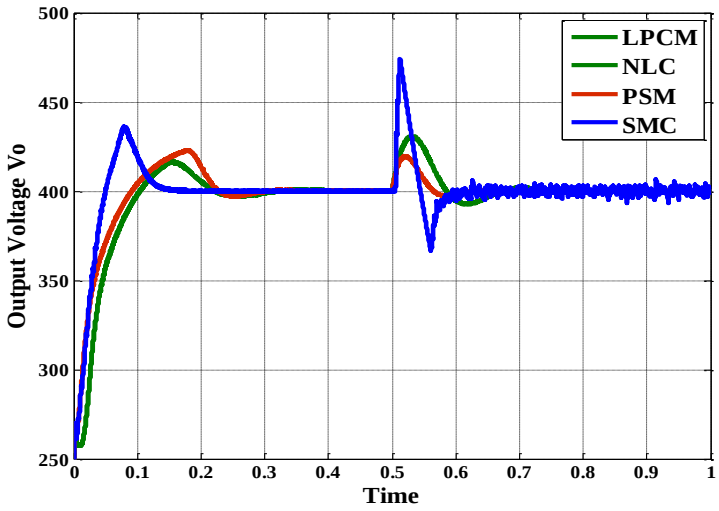

Figure 13. Comparison of SMC output voltage of IFBC with PSM, NLC and LPCM controllers

Table 2. Comparison of SMC with other controllers

Controlling Scheme	Rise Time (t_r) sec.	%Peak Over shoot(Mp)	Settling Time (Ts) sec.	Steady State Error(e_{ss})
SMC	0.08	15	0.15	0
PSM	0.18	10	0.3	0
NLC	0.15	12	0.4	0
LPCM	0.15	12	0.4	0

6. CONCLUSION

In this paper an Isolated Full Bridge Boost Converter mostly used for fuel cell applications was presented and implemented in closed loop configuration. A robust control technique for controlling output voltage of converter known as Sliding Mode Control (SMC) was proposed and presented in detail. SMC was applied to the IFBC topology and the results obtained are compared with other controllers. From the comparison results it can be shown that faster transient response of the converter is achieved i.e the rise time and settling time has been improved and when a disturbance i.e load change has occurred the response of output voltage to reach the actual value is very fast with Sliding Mode Control. Inspite of these many advantages, the only disadvantage observed is the peak overshoot at load change which can be limited by designing any other advance controllers like H-infinity or ANFIS.

REFERENCES

[1] Amar Nath Mishra, Vijay Kumar Manjhi, Archana Soni, and K.Sudhakar, "Opportunities and Challenges for Fuel Cells in India," *International Journal of Advanced Research in Science and Engineering*, vol. 5, no. 6, Jun 2016.

[2] Vipin Das, Sanjeevi kumar Padmanaban, Karthikeyan Venkitusamy, Rajasekar Selvamuthukumaran, Frede Blaabjerg, and Pierluigi Siano, "Recent advances and challenges of fuel cell based power system architectures and control – A review," *Renewable and Sustainable Energy Reviews*, vol. 73, pp. 10–18, 2017.

[3] Emadi, S. S. Williamson, and A. Khaligh, "Power electronics intensive solutions for advanced electric, hybrid electric, and fuel cell vehicular power systems," *IEEE Trans. on Power Electronics*, pp. 567-577, 2006.

[4] Emadi, K. Rajashekara, S. S. Williamson, and S. M. Lukic, "Topological overview of hybrid electric and fuel cell vehicular power system architectures and configurations," *IEEE Trans. on Vehicular Technology*, pp. 763-770, 2005.

[5] A. Averberg, K. R. Meyer, C.Q. Nguyen, and A. Mertens, "A Survey of Converter Topologies for Fuel Cells in the kW Range," *Energy Conference, 2008 ENERGY. IEEE*, 2008.

[6] K. Rajashekhara, "Power conversion and control strategies for fuel cell vehicles," in *Proc. IEEE IECON*, 2003.

[7] X. Kong, L. T. Choi, and A. M. Khambadkone, "Analysis and control of isolated current-fed full bridge converter in fuel cell system," in *Proc.IEEE IECON*, vol. 3, pp.2825–2830, Nov 2004.

[8] S. Radhika, S. Swathi, and Sarfaraz Nawaz Syed "Design and Analysis of Current Mode Control of Boost Converter," *International Journal of Science and Research (IJSR)*, vol. 5, no. 1, Jan 2016.

[9] S. Dhanasekaran, E. Sowdesh Kumar, and R. Vijaybalaji, "Different Methods of Control Mode in Switch Mode Power Supply- A Comparison," *International Journal of Advanced Research in Electrical, Electronics and Instrumentation Engineering*, vol. 3, no. 1, Jan 2014.

[10] Saifullah Amir, Ronan v. d. Zee, and Bram Nauta, "An Improved Modeling and Analysis Technique for Peak Current Mode Control based Boost Converters," *IEEE transactions on power electronics*, 2015.

[11] Yosra Massaoudi, Dorsaf Elleuch, Driss Mehdi, Tarak Damak, and Ghani Hashim "Comparison Between Non Linear Controllers Applied to a dc-dc Boost Converter," *International Journal of Innovative Computing, Information and Control*, vol. 11, no. 3, Jun 2015.

[12] Steffi Selvaraj and K. Yasoda, M. E., "Optimization and Closed Loop Control of Soft Switched Boost Converter with Flyback Snubber," *International Journal of Computer Applications* (0975 – 8887), *International Conference on Innovations in Intelligent Instrumentation, Optimization and SignalProcessing ICIIIOSP*, 2013.

[13] L. Navinkumar Rao, Sanjay Gairola, Sandhya Lavety, and Noorul Islam, "Design of DC-DC Boost Converter with Negative Feedback Control for Constant Current Operation," *International Journal of Power Electronics and Drive System (IJPEDS)*, vol. 8, no. 4, pp. 1575-1584, Dec 2017.

[14] G. Seshagiri Rao, S. Raghu, and N. Rajasekaran, "Design of Feedback Controller for Boost Converter Using Optimization Technique," *International Journal of Power Electronics and Drive System (IJPEDS)*, vol. 3, no. 1, pp. 117~128, Mar 2013.

[15] Souvik Chattopadhyay, V. Ramanarayanan, and V. Jayashankar, "A Predictive Switching Modulator for Current Mode Control of High Power Factor Boost Rectifier," *IEEE Transactions on Power Electronics*, vol. 18, no. 1, Jan 2003.

[16] Santhosh T. K. and Govindaraju C., "Development of Predictive Current Controller for Multi-Port DC/DC Converter," *International Journal of Power Electronics and Drive Systems (IJPEDS)*, vol. 6, no. 4, pp. 683–692, Dec 2015.

[17] K. Ramalingeswara Prasad, P. Deepak Reddy, and Kranthi Kiran Ankam, "Boost Compensator for Predictive Current Mode Control of High Power Factor Boost Rectifier," *International journal of computer applications*, vol. 5, no. 2, Aug 2010.

[18] S. Vijaya Madhavi and G. Tulasi Ram Das, "Comparative Study of Controllers foe an Isolated Full Bridge Boost Converter Topology in Fuel Cell Applications," *International Journal of Power Electronics and Drive System (IJPEDS)*, vol. 9, no. 4, pp. 1644-1656, Dec 2018.

[19] Riccardo Pittini, Zhe Zhang, and Michael A.E. Andersen, "Isolated Full Bridge Boost DC-DC Converter Designed for Bidirectional Operation of Fuel Cells/Electrolyzer Cells in Grid-Tie Applications," *Proceedings of EPE '13-ECCE Europe*, Sep 2013.

[20] P.Mattavelli, L. Roossetto, and G. Spiazzi, "Unity Power Factor Control in Three-Phase AC/DC Boost Converter Using Sliding Modes," *IEEE Transactions on Industrial Electronics*, vol. 55, no. 11, pp. 3874-3882, Nov 2008.

[21] P. mattavelli, L. rossetto, and L. malesani, "Application of sliding mode control design to Switch-Mode Power Supplies," *Journal of Circuits, Systems and Computers (JCSC)*, vol. 5, no. 3, pp. 337-354, Sep 1995.
[22] R. A. Decarlo, S. H. Zak, and S. V. Drakunov, "Variable Structure, Sliding Mode Control Design," *Control System Hand Book*, pp. 941- 951.
[23] O. Lopez, L. Garacia de Vicuna, and M. Castilla "Sliding Mode Control Design of a Boost High- Power Factor pre-regulator vased on the Quasy- Steady-State Approach," *IEEE Trans.*, pp. 932-935, 2001.
[24] R. Anusuyadevi, P. Suresh Pandiarajan, and J. Muruga Bharathi, "Sliding Mode Controller based Maximum Power Point Tracking of DC to DC Boost Converter," *International Journal of Power Electronics and Drive System (IJPEDS)*, vol. 3, no. 3, pp. 321-327, Sep 2013.
[25] A. Safari and H. Ardi, "Sliding Mode Control of a Bidirectional Buck/Boost DC-DC Converter with Constant Switching Frequency," *Iranian Journal of Electrical & Electronic Engineering*, vol. 14, no. 1, Mar 2018.

BIOGRAPHIES OF AUTHORS

S.Vijaya Madhavi was born in India. She received her B.tech in the department of EEE (2005), from PVP Siddhartha Institute of Technology, Vijayawada India and M.tech (2007) in department of EEE, from Jawaharlal technological university Hyderabad. She has five years of teaching experience in JNTU affiliated colleges. Presently she is pursuing her PhD in department of EEE, Jawaharlal technological university Hyderabad. Her research interests include power electronic converters, renewable energy sources and controlling of SMPS.

Dr. G Tulasi Ram Das was born in the year 1960 in Hyderabad, Andhra Pradesh, India. He received his B.Tech, in Electrical & Electronics Engineering from JNT University Hyderabad in 1983 and M.E., in Industrial Drives and Controls from Osmania University, Hyderabad in 1986 and Ph.D., in Electrical Engineering from Indian Institute Of Technology, Madras in 1996. He was Vice-Chancellor, for JNTUK Kakinada, from Nov2011 to Nov2014. Presently he is Professor in department of EEE, JNT University Hyderabad. His research interests include Power Electronics, Power Semi-conductor controlled electric drives (IM, PMSM, & BLDCM), Resonant Converters, Multilevel Converters, Flexible AC Transmission Systems (FACTS), Power Quality and Solar PV Cell Technologies, and E-waste management. He has published 151 Research papers in Electrical Engineering at National and International Journals and Conferences. He is a member in editorial board of three journals.